International Journal Of
Industrial Electronics Control and Optimization
Print ISSN: 3517-2645
Online ISSN: 3568-2645
Homepage: https://ieco.usb.ac.ir/

Design A Novel Ultrasonic Horn Using Electro-Mechanical Circuit Method with Optimization Algorithm

Davoud Mirzaei [1] and Saeed Amini[†2]

Manufacturing Department, Faculty of Mechanical Engineering, University of Kashan, Kashan, Iran.[1,2]
Corresponding author's email: amini.s@kashanu.ac.ir

Article Info

Article type:
Research Article

Article History:
Received 2022-01-29
Received in revised form 2022-06-12
Accepted 2022-07-06
Published online:2022-09-18

Keywords:
Barbell Horn,
Electro-Mechanical Circuit,
PSO Optimization,
Ultrasonic Instrument.

ABSTRACT

In this paper, an ultrasonic horn based on the PSO algorithm for emulsion homogenization is optimized and fabricated. The application of various ultrasonic instruments such as horns in different industrial procedures is increasingly expanding and developing. Horn is a tool that has played a crucial role in the energy transfer to fluid. Longitudinal frequency, vibration amplitude, length-to-diameter ratio, a distance of frequency from other frequency modes, wide distribution of cavitation along with the horn's length, and increasing the area of acoustic energy transfer are the main characteristics of the horn design procedure. Therefore considering these important features with using the PSO algorithm and electro-mechanical circuit method to finding resonance frequency, the design procedure of the optimized horn is performed. The definition of the objective function is based on the horn's amplification factor, and the rest of the other characteristics are defined as design constraints. The simulation results show a 15% improvement in the natural frequency compared to the target frequency and a suitable frequency distance of 2.5 kHz between the previous and next modes. According to the barbell part of the horn, the amplification factor of 14 was obtained for the proposed horn, the frequency and amplitude of the vibration were evaluated. The experimental results were very close in terms of amplification factor and frequency to the simulation results with reasonable accuracy.

I. Introduction

High-power ultrasound has been used in many industrial processes such as cleaning, extraction, homogenizing, emulsification, sonochemistry, pollutant destruction, etc. These Processes are primarily based totally on the impact of acoustic cavitation made via way of means of ultrasonic horn vibration in water. This oscillation is produced by an electromechanical transducer, which is composed of piezoelectric elements that convert high-frequency voltage into mechanical oscillation. However, the amplitude of the transducer is not sufficient to cause cavitation. To transmit sound waves into the water, you need a rod horn of a different shape.

One of the most important challenges in using ultrasonic horns on an industrial and semi-industrial scale is propagating an acoustic wave with a high vibration amplitude throughout the fluid or emulsion. Widespread cavitation production all over the liquid increases the efficiency of emulsification. To this end, extensive research has been conducted on the design of high-power ultrasonic horns. The three main goals in increasing efficiency are to increase the amplitude of vibration and increase and distribute emission area along with the horn.

High-amplitude horns are used in various ultrasonic applications such as ultrasonic operation, ultrasonic motors, ultrasonic lubrication, ultrasonic homogenizing, and ultrasonic welding. According to different horn shapes, ultrasonic horns can be divided into stepped, exponential, conical, catenary, and bezier. Moreover, there is specialized complex hybrid ultrasonic horn such as cylindrical with cuboid hole, multi-Step, double conical, cylindrical conical exponential, cylindrical double exponential horn, barrel,

DOI : 10.22111/IECO.2022.41457.1409

barbell, spool-shaped, double conical stepped, double conical cylindrical, multistep conical, etc. Each type has advantages and disadvantages [1].

Use of ultrasonic transducers is common in various applications, including machining [2-3], burnishing [4], emulsion of solutions, flotation improvement in the mining industry, Friction Stir Welding, etc. During recent decades studies on the development of ultrasonic horns have been done. One part of the study is analytical modeling [1,5-7] , and another part is numerical [8–10].

One type that suggests homogenizing emulsion is the barbell horn. Previous studies on barbell horns have been done for modeling and optimization horns. Peshkovsky [11-13] developed a novel type of high-power ultrasonic transducer, which has a large radiating surface and high amplification factor. Peshkovsky and colleagues [14] published a report on CBD Nanoemulsions stabilized by tween80/span80. The report was created with a laboratory-scale ultrasonic liquid processor; they also demonstrated the scalability of the emulsification process. Fu [15] developed a full-wave rod horn with longitudinal vibration, which helps to improve the sound energy transmission of the ultrasonic vibration system working in the longitudinal vibration mode, and obtains the resonance frequency equation.

Heikkila studies have done much to optimize ultrasonic horn. The interactive multiobjective optimization method NIMBUS is applied in designing a high-power ultrasonic transducer. The performance of the transducer is simulated with a finite element model, and three design goals are formulated as objective functions to be minimized [16]. Deibel and Wegener [17] proposed a multi-dimensional optimization numerical method for stepped double-flanged horns. This method uses genetic algorithms to determine the basic shape of the horn and then uses the simplex method to further optimizing the shape. Zohourmesgar [18] checked the optimization based on temperature increase, which would change its mechanical properties and significantly reduce the resonance frequency and vibration efficiency. In addition, the thermal optimization of the horn is carried out in two steps with the idea of fins using genetic algorithms. Roşca [19] proposed a shape optimization method that takes into account the stiffness of the contact between the horn and the connected instrument. It is considered to be the objective function of minimizing the volume under the condition of structural equilibrium. Rosca [20] developed and characterized an ultrasonic horn with a given operating frequency, gain, and node position, and effectively used theories, experiments, and calculation methods for this purpose. Afshari and Arezoo [21] proposed a dual-purpose method for optimizing the wide horn topology. This is for two purposes: the longitudinal natural frequency of the horn should be similar to the frequency of the adjustable transducer amplifier, and the output surface of the horn should vibrate uniformly. Afshari and Arezoo [22] use factors such as the regularity of vibration amplitude, longitudinal natural frequency, frequency spacing, magnification, and maximum stress of the horn body. The problems With using genetic algorithm and boundary condition processing methods, a block horn optimization design method was investigated. Kumarasami [23] is studying the design and optimization of slotted horns used in the ultrasonic insertion process through integrated response surface method (RSM), finite element analysis (FEA), and genetic algorithm (GA). He [24] based on the genetic algorithm, by optimizing the control points at the start and end of the Bezier curve, a horn with a large amplitude ratio is obtained. Yu [25] proposed a systematic method for optimizing and adjusting the target natural frequency of the horn at high temperatures. The numerical results show that the longitudinal natural frequency of the horn decreases significantly with the increase of the mold temperature. YN [26] assumes that the ten-element horn is modeled by the electromechanical equivalent circuit method and retains the longitudinal vibration of the HPU transmitter. The resonance frequency equation and structure size are also optimized for the longitudinal vibration. Zuguo et al. [27] optimization design method coupled finite element genetic algorithm and heat for the ultrasonic oscillator is proposed. In Wei and Weavers's study [28], a multi-stepped ultrasonic horn with a coned tip was analytically designed, and its sonochemical performances were effectively enhanced. Additionally, special ultrasonic block horns with slots or island arrays were optimally designed to achieve uniform amplitudes at their work. Based on the studies regarding the ultrasonic horns, the material and design of horn geometric shape, determine its magnification factor [29].

In this paper optimization barbell horn has done with purpose increasing amplitude and cross-section with adding multistep in the end part of the horn . For this purpose have used impedance equivalent circuits to calculating frequency and amplification factors and constraints have considered for geometrical parameters.

The paper is organized as follows. The proposed structure of the ultrasonic barbel horn and equivalent circuit are discussed in Section 2. A brief overview of the PSO algorithm is presented in Section 3. Shape optimization of the proposed barbell horn based on PSO algorithm is done in section 4. Finite Element model and Experimental procedure and materials is presented in section 5 and 6. Results evaluation and discussion are in section 7. In the end, the concluding remarks are drawn.

II. The proposed structure of the ultrasonic barbell horn

For access to high vibration amplitude in emulsification, a barbell horn was invented. This horn has five elements that

are designed based on full wavelength. High gain factor and increasing the propagation area of ultrasonic waves are original targets for the invention barbell horn. Moreover propagation acoustic waves of the cross-sectional area of the horn cause increasing diffusion and energy efficiency so barbell horn structure to 9 elements Fig.1 has increased topological changes to the structure occur in five elements Such that multi-step add to the Fifth element.

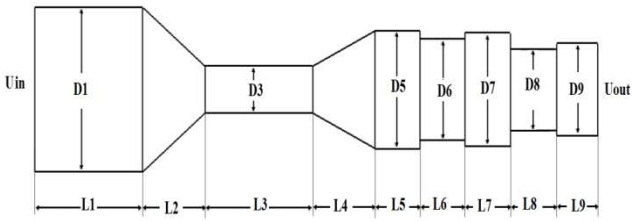

Fig.1. Multi Step barbell Horn

Another characteristics of this horn is that the maximum amplitude is not at the end of the horn, but we will also have the maximum amplitude along with the horn. This is an opportunity that ultrasonic emission zones cannot be concentrated in just one area but extended along the horn to increase efficiency and effectiveness. In the proposed horn structure, an attempt has been made to create steps at the end of the barbell horn to increase the cavitation areas in the emulsion homogenization. Therefore, an attempt was made to change the geometric parameters with the optimization and numerical solution algorithm to achieve the desired goal.

III. Equations of Vibration of the horn for each element and gain factor

The suggested horn has nine elements that for calculating gain factor need to solve the equation of vibration for each element in Equ. (1).

$$\frac{d^2u}{dx^2}+\frac{1}{A(x)}\frac{dA}{dx}\frac{du}{dx}+k^2u=0 \quad (1)$$

where k = ω/c is the wave number, ω = 2πf is the angular frequency of vibrations, c is the velocity of sound in the material, f is the frequency of vibrations and A(x) is the position dependent cross sectional area. The radius change along the horn $\alpha=\frac{r_1-r_2}{Lr_1}$ is defined (r_1 is radius at the beginning and r_2 at the end of the horn) and L is its length. The relation of the cross section area of the cone at different distances x will was $A_x=\pi {r_x}^2=\pi {r_1}^2(1-\alpha x)^2$. Because of the geometrical difference between cylindrical and conical horn, it is needed to drive equations individually. So the solutions have presented in Equ. (2) .Each element has independent coordinates system and solve based on the condition of continuity of force and speed in boundary points.

$$\begin{aligned}
u_1 &= A_1\cos kx + B_1\sin kx && 0<x<L_1\\
u_2 &= F_2(A_2\cos kx + B_2\sin kx) && 0<x<L_2\\
u_3 &= A_3\cos kx + B_3\sin kx && 0<x<L_3\\
u_4 &= F_4(A_4\cos kx + B_4\sin kx) && 0<x<L_4\\
u_5 &= A_5\cos kx + B_5\sin kx && 0<x<L_5\\
u_6 &= A_6\cos kx + B_6\sin kx && 0<x<L_6\\
u_7 &= A_7\cos kx + B_7\sin kx && 0<x<L_7\\
u_8 &= A_8\cos kx + B_8\sin kx && 0<x<L_8\\
u_9 &= A_9\cos kx + B_9\sin kx && 0<x<L_9
\end{aligned} \quad (2)$$

Then, using the boundary conditions for the horn's elements, the system of equations for displacements ($u_1 \ldots u_9$), is obtained. Therefore, gain factor of the horn can be expressed as Equ. (3) [11].

$$G=\left|\frac{u_{out}}{u_{in}}\right|=\frac{A_9\cos kL_9+B_9\sin kL_9}{A_1\cos kx+B_1\sin kx} \quad (3)$$

IV. The Impedance equivalent circuit and resonance frequency equations of the horn

In designing and analyzing the vibrational characteristics of elastic mechanical elements The electro-mechanical equivalent circuit model has been proven to be very useful method. One of most important vibration characteristic is resonance frequency that with this method calculates analytically. The equivalent circuit Based on the transmission line theory for the horn can be obtained With Considering force and velocity continuity conditions at the boundaries of the nine elements of the horn [30].

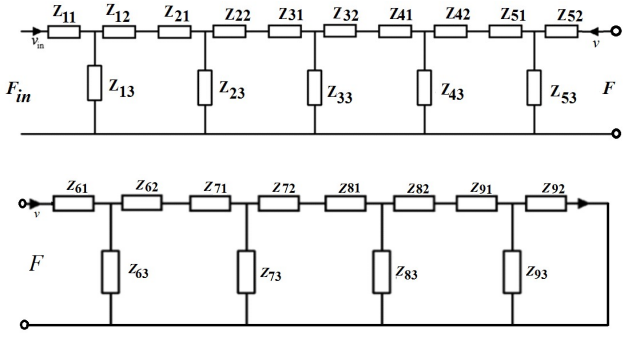

Fig. 2 electro-mechanical equivalent circuit of multi-step barbell horn

The multi-step barbell horn consists of nine elements, including six constant cross-section cylinders and two conical cross-section rods connected in series mechanically. The equivalent circuit of the nine-element barbell horn can be obtained based on conical metal rod and a constant cross section metal rod (Fig.2). The expressions for the impedances of the nine elements are as follows Equ. (4) to Equ. (23).

$$z_{11}=z_{12}=jz_1\tan(kl_1/2) \quad (4)$$

$$z_{13}=-jz_1/\sin kl_1 \quad (5)$$

$$z_{21} = jz_2\left(\frac{N_2-1}{N_2kl_2}+\frac{1}{N_2\sin\ kl_2}-\frac{1}{\tan\ kl_2}\right) \quad (6)$$

$$z_{22} = \frac{jz_2}{N_2}\left(\frac{1}{\sin\ kl_2}-\frac{N_2-1}{N_2kl_2}-\frac{1}{N_2\tan\ kl_2}\right) \quad (7)$$

$$z_{23} = -\frac{jz_2}{N_2\sin\ kl_2} \quad (8)$$

$$z_{31} = z_{32} = jz_3\tan\,(kl_3/2) \quad (9)$$

$$z_{33} = -jz_3/\sin\ kl_3 \quad (10)$$

$$z_{41} = jz_4\left(\frac{N_2-1}{N_2kl_4}+\frac{1}{N_2\sin\ kl_4}-\frac{1}{\tan\ kl_4}\right) \quad (11)$$

$$z_{42} = \frac{jz_2}{N_2}\left(\frac{1}{\sin\ kl_4}-\frac{N_2-1}{N_2kl_4}-\frac{1}{N_2\tan\ kl_4}\right) \quad (12)$$

$$z_{43} = -\frac{jz_2}{N_2\sin\ kl_4} \quad (13)$$

$$z_{51} = z_{52} = jz_5\tan\,(kl_5/2) \quad (14)$$

$$z_{53} = -jz_5/\sin\ kl_5 \quad (15)$$

$$z_{61} = z_{62} = jz_1\tan\,(kl_6/2) \quad (16)$$

$$z_{63} = -jz_1/\sin\ kl_i \quad (17)$$

$$z_{71} = z_{72} = jz_7\tan\,(kl_7/2) \quad (18)$$

$$z_{73} = -jz_7/\sin\ kl_i \quad (19)$$

$$z_{81} = z_{82} = jz_8\tan\,(kl_8/2) \quad (20)$$

$$z_{83} = -jz_8/\sin\ kl_8 \quad (21)$$

$$z_{91} = z_{92} = jz_9\tan\,(kl_9/2) \quad (22)$$

$$z_{93} = -jz_9/\sin\ kl_9 \quad (23)$$

where

$z_{11}, z_{12}, z_{13}, z_{31}, z_{32}, z_{33}, z_{51}, z_{52}, z_{53}, z_{61}, z_{62}, z_{63}, z_{71}, z_{72}, z_{73}, z_{81}, z_{82}, z_{83}, z_{91}, z_{92}, z_{93}$ are mechanical impedances of cylindrical elements and z_{21}, z_{22}, z_{23}, z_{41}, z_{42}, z_{43} are mechanical impedances of conical elements. In impedance relations

$z_1 = \rho cS_1,\ z_2 = \rho cS_2,\ z_3 = \rho cS_3,, z_4 = \rho cS_4,\ z_5 = \rho cS_5, z_6 = \rho cS_6, z_7 = \rho cS_7, z_8 = \rho cS_8, z_9 = \rho cS_9 N_4 = \frac{d_2}{d_4}, N_2 = \frac{d_1}{d_2}, S_1 = \pi(d_1/2)^2, S_2 = \pi(d_1/2)^2,\ S_3 = \pi(d_3/2)^2, S_5 = \pi(d_5/2)^2, S_4 = \pi(d_3/2)^2$ sound speed and wave-number to the longitudinal vibration $c = \sqrt{E/\rho}$ and $k = \frac{\omega}{c}$ and ρ, E, and σ are density, Young's modulus, Poisson's ratio of longitudinal vibration .

Acoording to impedance relation equivalent impedance is Z = R + jX that R is real part of impedance (resistance) and X is imaginary part of impedance (reactance) . for find resonance frequency solve reactance equation as follows:

$$\mathrm{Im(Z)} = X = 0 \quad (24)$$

This relation depends on material and geometrical parameters of horn. So this has used in optimization for investigating domain frequency.

V. particle swarm optimization (PSO)

Particle swarm optimization (PSO) is a computational method that optimizes a problem by iteratively trying to improve a candidate solution with regard to a given measure of fitness. The PSO is a proposed metaheuristic method that simulates a stylized representation of the movement of organisms in a bird flock or fish school. The standard PSO algorithm works by having a swarm of particle's, a population of candidate solutions, which move around in the search space according to the particle's position and velocity [31-32].

This method can be defined as a group of birds randomly searching for food in an area and there is food only in one part of the search area. None of the birds know the location of the food, but they know the distance to the food at each stage of the search. The question now is what is the best way to get to food? Perhaps the most effective strategy is for the birds to follow the bird that is closest to the food.

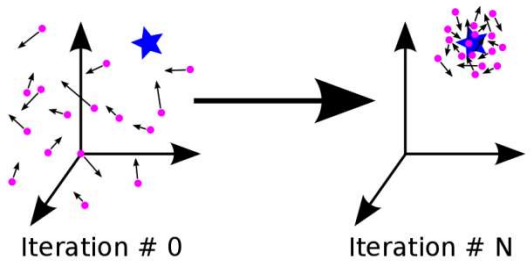

Fig. 3 Mechanism of finding the answer to the problem in the particle swarm method [31]

In PSO algorithm, the group of particle's in search space purpose to optimize a fitness function, in an approach like to movement of flocks of birds in natural environment in search of food. The particle's are positioned randomly in search space and they calculate their suitability at that position. Then, for a predefined number of iterations, each particle changes to a new location which provides better fitness than the earlier position. This program is based on the history of particles own best and current locations with those of the best positions achieved by other particle's in the swarm, with some chance perturbations. Thus in following iterations the swarm reaches the most optimum solution to the fitness function in the problem space, with a defined number of particle's employed together. The fitness or objective function in PSO algorithm is a performance evaluation criterion that depends on the application area of the algorithm. The performance principle is usually defined by a mathematical formulation to compute the system performance achieved through a performance index.

The algorithm first starts with a randomly initialized population of particle's and updates with iterations and generates new positions, and searches for the optimal point. If population size is assumed to be N particle's, the i^{th} particle in iteration t and in ant m dimension search space, has three properties.

The i^{th} particle has position $\mathrm{X_i(x_{i1}, x_{i2}, \dots, x_{im})}$ and velocity $\mathrm{V_i(v_{i1}, v_{i2}, \dots, v_{im})}$. And $\mathrm{x_{pbest}}$, $\mathrm{x_{gbest}}$ represents

personal best position and global best position of ith particle. At first iteration, the personal best position will be updated to the current position of the particle and the personal best position at t+1 iteration will be $\mathrm{x}_{\mathrm{pbest}_{\mathrm{i}}}(\mathrm{t}+1)$

$$x_{pbest_{\mathrm{i}}}(\mathrm{t}+1) = \begin{cases} x_{pbest_{\mathrm{i}}}(\mathrm{t}) & \mathrm{f}(\mathrm{x_i}(\mathrm{t}+1)) \geq \mathrm{f}\left(x_{pbest_{\mathrm{i}}}(\mathrm{t})\right) \\ x_{pbest_{\mathrm{i}}}(\mathrm{t}) & \mathrm{f}(\mathrm{x_i}(\mathrm{t}+1)) < \mathrm{f}\left(x_{pbest_{\mathrm{i}}}(\mathrm{t})\right) \end{cases} \quad (25)$$

After the best individual position of the i[th] particle in the t iteration was determined, It is easy to determine the best position ever seen among all the population particle's. This position with x_{gbest} has shown that to obtain it, the best individual position of the whole N particle is observed up to the t iteration with $P(t)$ relation

$$P(t) = \left\{x_{pbest_1}(t), x_{pbest_2}(t), \dots, x_{pbest_N}(t)\right\} \quad (26)$$

The best position found by the whole population particle's up to the t iteration of the algorithm is obtained using Equ. (27).

$$\mathrm{f}(x_{gbest}(\mathrm{t})) = min\left\{\mathrm{f}\left(x_{pbest_{\mathrm{i}}}(\mathrm{t})\right) \mid x_{pbest_{\mathrm{i}}}(\mathrm{t}) \in \mathrm{P}(\mathrm{t})\right\} \quad (27)$$

In the t iteration of the PSO algorithm, the position of the i[th] particle is X_i^t, which is updated by the vector V_i^{t+1} and the i particle finds the new position X_i^{t+1} according to the Equ. (28).

$$V_i^{t+1} = wV_i^t + c_1r_1\left(x_{pbest} - X_i^t\right) + c_2r_2\left(x_{gbest} - X_i^t\right)$$
$$X_i^{t+1} = X_i^t + V_i^{t+1} \quad (28)$$

So the position of the updated particle X_i^{t+1} of the four factors of the current position X_i^t, the current velocity V_i^t, the distance between the current position and the best individual position $(x_{pbest} - X_i^t)$ and the distance between the current position and the best position Social $(x_{gbest} - X_i^t)$ follows.

In this relation, the values r1 and r2 are random numbers with uniform distribution in the range (1,0), C1 is related to $(x_{pbest} - X_i^t)$ and C2 is related to $(x_{gbest} - X_i^t)$. Therefore, C1 and C2 are called individual and social cognition parameters, respectively. In the above relation, C1 determines the maximum amount of particle motion towards the best individual position of the particle and C2 determines the maximum amount of particle motion towards the best social position. In the above relation, in order to better explore the search space, they limit the movement speed between the intervals [-vmax, vmax]. This causes the particle to move a little slower towards the best response as it moves, so that if there is a better response in the distance between the particle and the best t iteration response, the particle will find that answer

VI. Shape optimization of the proposed barbell horn based on PSO algorithm

The barbell horn is one of the most widely used ultrasonic horns. The geometric dimensions of the barbell horn have a direct effect on its performance in producing ultrasonic waves. Determining the geometric dimensions of the barbell horn to achieve the desired performance using analytical methods is very complex and there is an approximation like the results. The use of numerical analysis methods such as Abacus software in the design of the barbell horn leads to more accurate results, but the shape design procedure is done by trial and error, which is very time-consuming and has local optimal results.

Therefore, the PSO algorithm can be used effectively in design the shape of the barbel horn, by defining the design procedure in the form of a suitable optimization problem. In determining the optimal shape of the proposed barbell horn, minimizing the amount of frequency, minimizing vibration, and increasing the voltage are very important. According to these goals and the structure of the barbell horn, the optimization problem for the shape design procedure is defined according to Equ. (29).

When the goal of the problem is more than one objective, such as optimizing the horn, we are faced with a multi-objective problem. In this case, since the frequency range of the horn is a priority due to the limitation of using transducers and generators to stimulate the horn, it has been determined as the initial condition and primary goal in the algorithm. Therefore, at this step, the particle population is evaluated in terms of frequency and particle's that are not in the frequency range are replaced with new random particle's. The process of the algorithm continues as standard with the evaluation of the horn interest and is shown schematically in Fig. 4.

$$Find:\ X_H = [l_1, l_2, \dots, l_9, d_1, d_3, d_5, \dots, d_9]^T$$
$$Maximaize:\ F_c(X_H) = \left|\frac{U_{out}}{U_{in}}\right|$$
$$Subjected\ to: \begin{cases} 19{,}500\mathrm{Hz} < f < 20{,}500\mathrm{Hz} \\ d_1 = 50mm, \\ 1 < d_1/d_3 < 5 \\ 0.5 < d_5/d_1 < 2 \\ 1.1 < d_{5,7,9}/d_{6,8} < 1.5 \\ l_1 + l_2 + \cdots + l_9 = \lambda \\ 10\mathrm{mm} \leqq L_1, L_3 \leqq 50\mathrm{mm} \\ 10\mathrm{mm} \leqq L_2, L_4 \leqq 30\mathrm{mm} \\ 10\mathrm{mm} \leqq L_5, L_6, L_7, L_8, L_9 \leqq 30\mathrm{mm} \end{cases} \quad (29)$$

where X_H represents the design vector for the implementation of the optimal shape design procedure. According to the structure of the proposed barbel horn in the

previous section, the longitudinal dimensions and diameters are indicated by l_i and d_i. The wavelength is indicated by λ. The components of the objective function, f_i, are defined according to Equs. (30) – (31).

$$f_1(X_H) = \frac{|\bar{u}_{zend}|}{|\bar{u}_{z1}|} \tag{30}$$

$$f_2(X_H) = \frac{|f_{nominal} - f\ |}{f} \tag{31}$$

Equ.30 being the amplitude ratio between input ($\bar{u}_{z1}$) and output ($\bar{u}_{zend}$) and Equ.31 consider difference frequency between nominal frequency ($f_{nominal}$) and frequency (f).

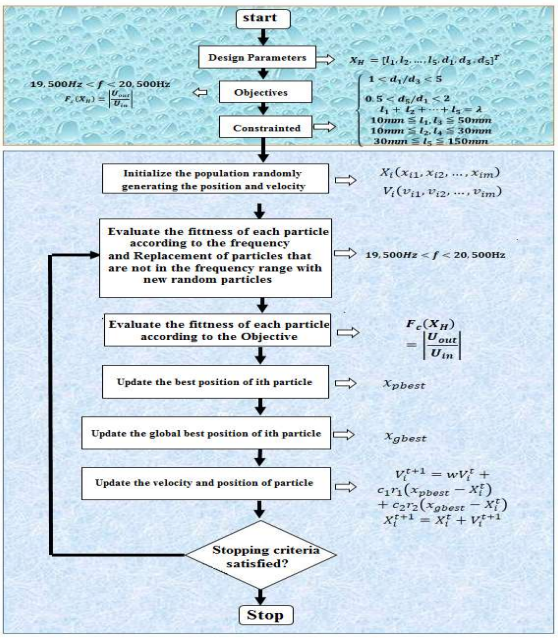

Fig. 4 Pso optimization algorithm

The Fig. 4 shows the PSO modified algorithm, so that that before checking the population, its frequency must be calculated. If it was in the specified frequency range, it will continued, otherwise, a new random population will replaced.

VII. Finite element model

One of the most effective and efficient methods for designing and evaluating the shape of a horn is using the numerical method. The numerical solution has very high accuracy but is relatively slower than the analytical method. The finite element method, like Abacus software, is a method for numerical solutions and offers approximate solutions to many complex engineering problems. Using the finite element method (FEM), any type of geometry can be studied; Such as deformation of members or geometry of elements, which is usually very difficult to use analytical methods.

Optimization does by Modal analysis that determines the natural frequencies and the mode shapes by solving the Eigenvalue equation as follows

$$(k - w_i^2 M)\Phi_i = 0 \tag{32}$$

where K is the global stiffness matrix, M is the global mass matrix, Φi is ith eigenvector, and wi is ith circular natural frequency. 3D model of the ultrasonic stack is developed in Abaqus software. Block Lanczos method is selected to compute the natural frequencies and mode shapes in the frequency range between 16 kHz and 25 kHz. The horn and booster are meshed by the C3D10 element (10-node quadratic tetrahedron element) with a different mesh size such that mesh size does not affect results.

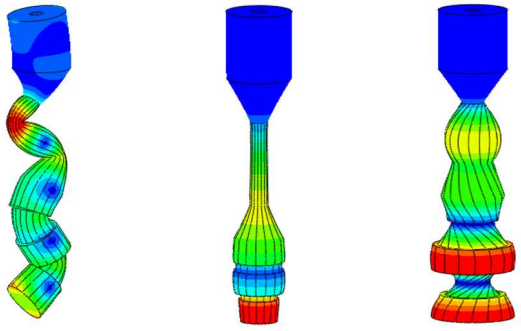

17.567 kHz 19.996 kHz 21.238 kHz

Fig. 5 Mode shapes of the ultrasonic optimized Horn near target frequency

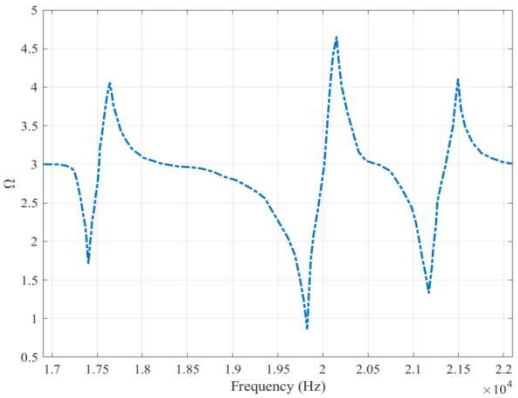

Fig. 6 Spectrum frequency Analysis of optimized horn

To determine the maximum stress value in the horn body and output peak-to-peak vibration amplitude of tip and different horn positions in a frequency equal to the longitudinal natural frequency of horn in the longitudinal direction do harmonic analysis. So in loop optimization use of two-step frequency and harmonic analysis in abaqus direct-solution steady-state dynamic analysis is utilized to calculate the stress value.

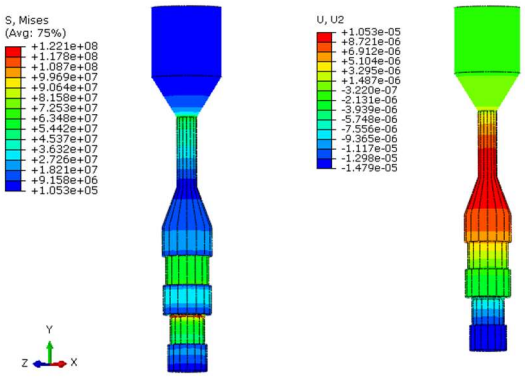

Fig. 7 Stress distribution and Displacement Amplitude in the optimized horn body

Stress distribution in Fig. 5 for optimized Horn is given. Stress maximum has occurred in point step which is considered to increase cavitation in the emulsion. Therefore, the maximum stress value will not be in the range of 316 steel fatigue stress. Due to the high-frequency dynamic load for any horn, infinite life can not be imagined.

Vibration Amplitude in the longitudinal direction of the optimized horn in Fig. 6 is given. Input amplitude in the first cross-section horn in harmonic step was 1(μm) that is amplified by the horn to 14.7 (μm) in the tip of the horn. So amplification factor of the optimized horn is 14.7.

Furthermore, the frequency difference between the longitudinal mode with the nearest previous and next modes are 2439 Hz and 1232 Hz, respectively. This shows that the frequency separation is more than 1 kHz.

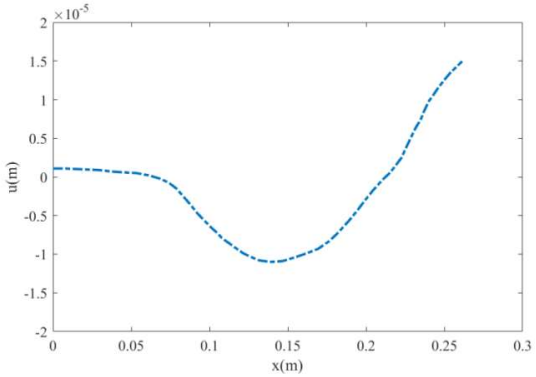

Fig. 8. Displacement amplitude of optimized multistep barbell horn

VIII. Experimental procedure and materials

To test the vibration amplitude and frequency of the manufactured results from the optimization, sensor eddy current (gap-sensor model AEC 5502A-01) has been used. Vibrations are measured at the tip of the horn and compared with harmonic analysis of Abaqus and calculated gain factor in experimental 14.83 and in numerical solution was 14.73 (Table 1). Operating power for the transducer is provided by a generator with a maximum output of 500W. The generator regulates the power output based on the selected amplitude setting and is designed for 20kHz. To check the frequency of the longitudinal mode of each result, used of high-precision commercial ZX70A impedance analyzer Fig. 10. The material used for manufacturing the ultrasonic devices is S316 with a Young's modulus of E = 193 GPa, υ = 0.285, ρ = 8000 (kg / m3) Poisson ratio of 0.3, and damping ratio of 1%. Material properties used in the FEM analysis are set accordingly. As shown in the Table 1, the experimental frequency and numerical difference of 4%.

TABLE 1
COMPARE EXPERIMENTAL AND NUMERICAL GAIN FACTOR

Gain Factor (Experimental)	Gain Factor (Numerical)	Gain Factor (Analytical)
14.83	14.73	15

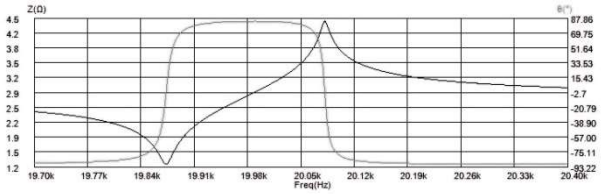

Fig. 9. amplitude and phase measurements with standard values

Fig. 10. Generating impedance curve by high-precision commercial ZX70A impedance analyzer

TABLE 2
COMPARE EXPERIMENTAL AND NUMERICAL FREQUENCY

Natural Frequency (Experimental)	Natural Frequency (Numerical)	Relative Variation (%)
20081	19996	0.04

IX. Conclusions

One of the most important challenges in designing an ultrasonic horn is determining its optimal dimensions. In the present study, the dimensions of a barbell horn were optimized to improve the vibration amplitude and surface area of the ultrasonic wave propagation. In the proposed, designed procedure, special attention was paid to the frequency and gain factor. Solving vibration equations of proposed horn with nine element and continuity force and velocity in boundary has arrived to gain factor. For finding

resonance frequency has used electro-mechanical circuit method. The design process was performed with MATLAB software and with optimization algorithm PSO. With the proposed method, the natural frequency was 0.15 higher than the target frequency and the distance between the frequency of the previous and next shape modes was about 5 kHz. The vibration amplitude coefficient, which is the ratio of the output amplitude to the input, increased to 14. The maximum stress with safety factor 2 was in the range. Experimental and numerical results showed little relative error. According to the comparative criterion of power coefficient, the optimized barbell horn had better performance and a larger wave propagation area, which led to better efficiency.

REFERENCES

[1] K. Mughal, M. Qureshi, A. Qaiser, and F. Khalid. Numerical Evaluation of State of the Art Horn Designs for Rotary Ultrasonic Vibration Assisted Machining of Nomex Honeycomb Composite. pp. 7–9, 2021. https://doi.org/10.21203/rs.3.rs-207300/v1

[2] S. Sajjady, H. Abadi, S. Amini, R. Nosouhi. Analytical and experimental study of topography of surface texture in ultrasonic vibration assisted turning. Materials & Design, 93:311-323.2016. https://doi.org/10.1016/j.matdes.2015.12.119

[3] Amini S, Aghaei M, Lotfi M, Hakimi E. Analysis of linear vibration in rotary turning of AISI 4140 steel. International Journal of Advanced Manufacturing Technology 91.2017. https://doi.org/10.1007/s00170-017-0108-5

[4] R. Teimouri, S. Amini. Analytical modeling of ultrasonic surface burnishing process: evaluation of through depth localized strain, International Journal of Mechanical Sciences,151,118-132.2019.https://doi.org/10.1016/j.ijmecsci.2018.11.008.

[5] J. G. Zhang, Z. L. Long, W. J. Ma, G. H. Hu, and Y. M. Li. Electromechanical dynamics model of ultrasonic transducer in ultrasonic machining based on equivalent circuit approach. Sensors (Switzerland),19, 6. https://doi.org/10.3390/s19061405

[6] V. I. Babitsky and J. Wittenburg. Foundations of Engineering Mechanics, 2012.

[7] S. G. Amin, H. A. Youssef. Computer-aided design of acoustic horns for ultrasonic machining using finite-element analysis,55: 254–260. 1995. https://doi.org/10.1016/0924-0136(95)02015-2.

[8] D. Lee and W. Cai. The effect of horn knurl geometry on battery tab ultrasonic welding quality: 2D finite element simulations. J Manuf Process, 28: 428–441.2017. https://doi.org/10.1016/j.jmapro.2017.04.009

[9] S. Roy. Design of a circular hollow ultrasonic horn for USM using finite element analysis. Int. J. Adv. Manuf. Technol.,93:319–328.2017. https://doi.org/10.1007/s00170-016-8985-6

[10] D. P. Singh, S. Mishra, R. K. Porwal. Modal analysis of ultrasonic horn using finite element method. Mater. Today Proc.18:3617–3623.2019. https://doi.org/10.1016/j.matpr.2019.07.293

[11] S. L. Peshkovsky, A. S. Peshkovsky. Matching a transducer to water at cavitation: Acoustic horn design principles. Ultrason Sonochem, 14: 314–322. 2007. https://doi.org/10.1016/j.ultsonch.2006.07.003.

[12] A. S.Peshkovsky, S.Bystryak. Continuous-flow production of a pharmaceutical nanoemulsion by high-amplitude ultrasound: Process scale-up. Chem. Eng. Process. Process Intensif,82:132–136.2014. https://doi.org/10.1016/j.cep.2014.05.007

[13] A. S. Peshkovsky, S. L. Peshkovsky, S. Bystryak. Scalable high-power ultrasonic technology for the production of translucent nanoemulsions. Chem Eng Process Process Intensif vol 69,: 77–82. 2013. https://doi.org/10.1016/j.cep.2013.02.010

[14] S. Leibtag, A. Peshkovsky. Cannabis extract nanoemulsions produced by high-intensity ultrasound: Formulation development and scale-up. J Drug Deliv Sci Technol.60,:101953.2020. https://doi.org/10.1016/j.jddst.2020.101953

[15] Z. Fu, X. Xian, S. Lin, C. Wang, W. Hu, G. Li. Investigations of the barbell ultrasonic transducer operated in the full-wave vibrational mode. Ultrasonics, 52: 578–586. 2012. https://doi.org/10.1016/j.ultras.2011.12.006

[16] E. Heikkola, K. Miettinen, P. Nieminen. Multiobjective optimization of an ultrasonic transducer using NIMBUS. Ultrasonics, 44, 4: 368–380.2006. https://doi.org/10.1016/j.ultras.2006.04.004

[17] K. R. Deibel, K. Wegener. Methodology for shape optimization of ultrasonic amplifier using genetic algorithms and simplex method. Journal of Manufacturing Systems 32(4):523-528. 2013. https://doi.org/10.1016/j.jmsy.2013.05.010

[18] . M. Zohhormesgar, H. Safikhani, M. R. Sheykholeslami, S. Mazdak. Optimization of ultrasonic transducer horn geometry with vibrational-thermal performance improvement approach. Journal of Solid and Fluid Mechanics, 11 (1): 31-42. 2021. https://doi.org/10.22044/JSFM.2021.8874.3014

[19] I. C. Roşc, S. T. Chiriacescu, N. C. Creţu. Ultrasonic horns optimization. Phys Procedia 3, : 1033–1040. 2010. https://doi.org/10.1016/j.phpro.2010.01.133

[20] I. C. Rosca, M. I. Pop, N. Cretu . Experimental and numerical study on an ultrasonic horn with shape designed with an optimization algorithm. Appl Acoust 95, , 60–69. 2015. https://doi.org/10.1016/j.apacoust.2015.02.009.

[21] M. Afshari, B. Arezoo. Design of wide ultrasonic horns based on topology optimization. Eng Optim, 1–21.2021. https://doi.org/10.1080/0305215X.2021.1901285

[22] . M. Afshari, B. Arezoo, Optimal design and experimental validation of ultrasonic wide blade horn. Appl Acoust 182, 108254.2021. https://doi.org/10.1016/j.apacoust.2021.108254

[23] A. Kumarasamy, E. Sooriyamoorthy. Design and Optimization of Slotted Block Horn Utilized in Ultrasonic Insertion Process Through Rsm-fea-ga Integration Technique, 2021. https://doi.org/10.21203/rs.3.rs-260954/v1

[24] T. He, X. Q. Ye, and Y. Zhao. Optimization design for ultrasonic horn with large amplitude based on genetic algorithm. J Vibroengineering 17 3,. 1157–1168. 2015.

[25] . J. Yu, H. Luo, T. V. Nguyen, L. Huang, B. Liu, Y. Zhang. Eigenfrequency characterization and tuning of Ti-6Al-4V ultrasonic horn at high temperatures for glass molding," Ultrasonics 101, (2020),106-125. https://doi.org/10.1016/j.ultras.2019.106002

[26] Y-N An, T-S Jang, U Ahn. A method of optimum design

for a high-power ultrasonic radiator with ten elements. J Vib Eng Technol. 2021. https://doi.org/10.1007/s42417-020-00264-9

[27] Z. Wei, J. A. Kosterman, R. Xiao, G. Y. Pee, M. Cai, L. K. Weavers. Designing and characterizing a multi-stepped ultrasonic horn for enhanced sonochemical performance. Ultrason Sonochem, 27 , 325–333.2015. https://doi.org/10.1016/j.ultsonch.2015.05.013

[28] Z. Liu, X. Jin, J. Zhang, Z. Hao, J. Li. Design optimization and eigenfrequency tuning of ultrasonic oscillator of one-dimensional longitudinal vibration at high temperature for laser welding. The International Journal of Advanced Manufacturing Technology,1-19. 2022. https://doi.org/10.1007/s00170-021-08530-0

[29] S. A. Sajjady, M. Lotfi, S. Amini, H. Toutounchi, A. B. Bami. Improving the surface energy of titanium implants by the creation of hierarchical textures on the surface via three-dimensional elliptical vibration turning for enhanced osseointegration. Proceedings of the Institution of Mechanical Engineers, Part H: Journal of Engineering in Medicine, , 233 1226-1236.2019. https://doi.org/10.1177/0954411919878306

[30] L. Wang., V. Hofmann, F. Bai, J. Jin, J. Twiefel. A novel additive manufactured three-dimensional piezoelectric transducer: Systematic modeling and experimental validation. Mechanical Systems and Signal Processing. 2019 Jan 1;114:346-65. https://doi.org/10.1016/j.asoc.2012.03.068

[31] M. Juneja, SK. Nagar. Particle swarm optimization algorithm and its parameters: A review. In2016 International Conference on Control, Computing, Communication and Materials (ICCCCM) 2016 Oct 21 (pp. 1-5). IEEE. https://doi.org/ 10.1109/ICCCCM.2016.7918233

[32] Y. Shi Y, R. Eberhart. A modified particle swarm optimizer. In1998 IEEE international conference on evolutionary computation proceedings. IEEE world congress on computational intelligence (Cat. No. 98TH8360) 1998 May 4 (pp. 69-73). IEEE. https://doi.org/10.1109/ICEC.1998.699146

Davood Mirzaei was born in Esfahan, Iran. He received his B.S. degree in Mechanical Engineering from Malek-e-Ashtar University of Technology, Esfahan, Iran, in 2008, and his M.S. degrees in Mechanical Engineering from the Yazd University, Yazd, Iran, in 2010, respectively. From 2010 to 2016, he was with Subsea R&D, Esfahan, Iran. From 2016 to 2022, he work as a ultrasonic Researcher at the Kashan Univerity, Kashan, Iran.

Saeid Amini was born in Esfahan, Iran, in 1974. He received his B.S. degree from the Amir Kabir University of Technology, Tehran, Iran, in 1998. He received his M.S. degree from the Esfahan University of Technology, Esfahan, Iran, in 2000 and Ph.D degree in Mechanical Engineering from the Tarbiat Modares University, Tehran, Iran, in 2008, respectively. In 2010, he joined the University of Kashan, as an Assistant Professor in the Department of Mechanical Engineering, where he was an Associate Professor from 2015 to 2020, and where he has been a Professor since 2020.